AIP Applied Physics Letters

Seebeck coefficient in silicon nanowire arrays

Emiljana Krali and Zahid A. K. Durrani

Citation: Applied Physics Letters **102**, 143102 (2013); doi: 10.1063/1.4800778
View online: http://dx.doi.org/10.1063/1.4800778
View Table of Contents: http://scitation.aip.org/content/aip/journal/apl/102/14?ver=pdfcov
Published by the AIP Publishing

Advertisement:

Re-register for Table of Content Alerts

Create a profile.

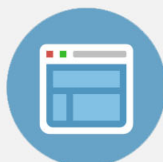

Sign up today!

This article is copyrighted as indicated in the abstract. Reuse of AIP content is subject to the terms at: http://scitation.aip.org/termsconditions. Downloaded to IP: 155.198.134.118 On: Tue, 22 Oct 2013 13:01:45

CrossMark

Seebeck coefficient in silicon nanowire arrays

Emiljana Krali and Zahid A. K. Durrani[a)]
Department of Electrical and Electronic Engineering, Imperial College London, South Kensington Campus, London SW7 2AZ, United Kingdom

(Received 15 October 2012; accepted 25 March 2013; published online 8 April 2013)

We measure the Seebeck coefficient S in large arrays of lightly doped n-Si nanowires (SiNWs). Our samples consist of $\sim 10^7$ NWs in parallel, forming a "bulk" nano-structured material. We find that the phonon drag component of S, a manifestation of electron-phonon scattering in the sample, is heavily suppressed due to surface scattering, and that there is a "universal" temperature dependence for S. Furthermore, at room temperature, S is enhanced in the arrays by up to ~ 3 times in comparison to bulk Si. © *2013 American Institute of Physics*. [http://dx.doi.org/10.1063/1.4800778]

In recent years, there has been great interest in thermoelectric (TE) effects[1–4] for application in alternative "clean" energy sources and for more efficient utilisation of energy. TE materials, where a temperature difference ΔT is converted into an electric potential difference ΔV, are quantified using the dimensionless figure-of-merit[5] $ZT = S^2\sigma T/\kappa$, where $S = \Delta V/\Delta T$, σ, and κ are the Seebeck coefficient, electrical and thermal conductivity, respectively, at temperature T. A value of $ZT \sim 1$ is necessary for practical applications.[6] While conventional bulk TE materials such as Bi_2Te_3 require a compromise between S, σ, and κ, limiting ZT $\sim$ 1, in nanostructured materials these parameters may be varied quasi-independently[3,4,7,8] such that $ZT > 1$. Here, S can be increased by quantum confinement of electrons without excessively affecting σ and furthermore, κ may be reduced independently of the other parameters by either increased surface scattering of phonons or modification of the density-of-states.[7,9] As these effects depend primarily on the length scale, there is greater freedom in material choice, and TE devices in materials even with nominally poor ZT become feasible.

Bulk Si, the most widely used semiconductor and the basis of large-scale integrated circuits, has a poor $ZT \sim 0.01$, due to high thermal conductivity,[10] $\kappa = 150$ W/mK at 300 K. However, measurements on a single[3] Si nanowire (SiNW) and $\sim$100 SiNWs in parallel[4] have reported $ZT \sim 1$. Here, the NWs were defined in heavily doped (10^{19}–10^{20}/cm^3) material to maximise σ, and κ was strongly reduced $\sim$1 W/mK, either due to increased surface scattering[3] or thermoelastic effects.[4] These observations demonstrate the potential for Si TE devices, raising the possibility of increased functionality in Si, and direct integration of TE and electronic devices for energy scavenging.

In this paper, we measure the temperature dependence of S in samples consisting of $\sim 10^7$ vertically aligned SiNWs (Fig. 1) fabricated using metal-assisted chemical etching (MACE).[11,12] The process creates SiNWs from $\sim$30 to 400 nm in diameter, with large aspect ratio up to 1:3000. We use a transient temperature and voltage measurement technique, allowing direct measurement of S in thin (1 mm thickness) samples. We also use lightly doped ($\sim 10^{15}$/cm^3) n-type Si to reduce impurity scattering of electrons and phonons. At low doping levels, phonon drag is the dominant contribution to S at moderate to low temperatures[10] ($\sim$200–30 K). Unlike heavily doped SiNWs used in previous work,[3,4] our low doping levels disentangle impurity scattering from surface scattering and leave the NW dimensions as the main source of scattering.

The SiNWs (Fig. 1) were synthesised from a lightly doped n-type silicon (100) wafer (resistivity $\rho \sim$ 1-5 Ω cm, phosphorous doping from 5×10^{14} to 3×10^{15}/cm^3) using a two-step chemical etching process.[13,14] Here, an electroless deposition (galvanic exchange) process deposits Ag nanoparticles from $HF/AgNO_3/H_2O$ solution on the Si surface. The nanoparticles act as catalysts for subsequent etching of the NWs in $HF/H_2O_2/H_2O$ solution. The main part of Fig. 1 shows the cross-section through a 60 μm long SiNW array. The insets 1-3 show higher resolution images of three areas (circled), at $\sim$5, $\sim$30, and $\sim$60 μm depth. The NWs are vertically aligned, with parallel sidewalls over the full etch depth. Inset 3 shows the base of the array, where NWs join the unetched substrate, cleaved at an angle to the NW cross-section. The NW morphology is complex, with irregular cross-section. This consists of a columnar core $\sim$100–400 nm in width with vertically aligned attached ribs $\sim$30–100 nm in width. At least some of the ribs are poorly attached or may be

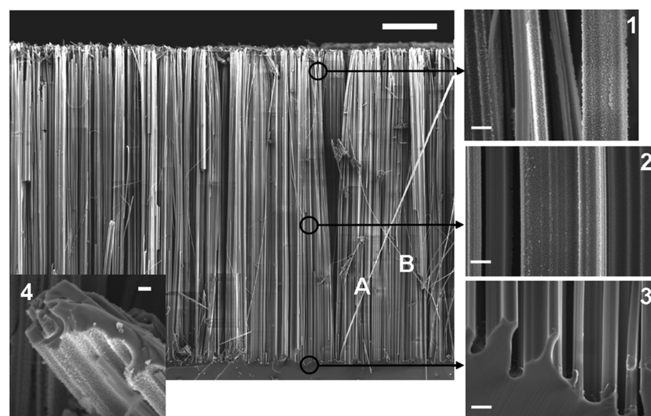

FIG. 1. Main image: Cross-sectional scanning electron micrograph through a 60 μm long SiNW array, obtained using a Zeiss Ultra Plus SEM. SiNWs marked "A" and "B" are $\sim$100 nm and $\sim$50 nm wide. The scale bar is 10 μm. Insets 1–3 show high-resolution micrographs of the corresponding circled regions. The scale bar is 200 nm. Inset 4 shows a broken-off section from the top of the array. The scale bar is 100 nm.

[a)]Electronic mail: z.durrani@imperial.ac.uk

This article is copyrighted as indicated in the abstract. Reuse of AIP content is subject to the terms at: http://scitation.aip.org/termsconditions. Downloaded to IP: 155.198.134.118 On: Tue, 22 Oct 2013 13:01:45

pinched-off, e.g., the NWs marked "A" (diameter ~100 nm) and "B" (diameter ~50 nm) may have broken off from a wider section. In each of our 0.5×0.5 cm^2 samples, using an array filling factor of ~30% and an average NW diameter of ~250 nm, there are ~10^7 NWs. The filling factor was extracted by measuring the change in sample weight after oxidation. Samples were oxidised at 1050 °C for several hours, completely oxidising the NWs. The change in sample weight allowed extraction of the weight of NWs. Using the NW weight, length, and density of Si, it is then possible to obtain the total cross-section area through the NWs and hence, the filling factor.

Insets 1-3 allow comparison of the NW surface roughness with array depth. This reduces from ~10 to 20 nm near the top (inset 1), to ~5 nm at ~30 μm depth (inset 2), to a negligible value at the bottom (inset 3). This suggests that the longer a section of NW surface remains immersed in the etchant, the greater the surface roughness due to increased surface etching. Inset 4 shows a broken-off section from the top of the array. While the NW surface roughness is ~20 nm, the core is unaffected.

S is measured using a transient temperature and voltage technique, allowing characterisation of thin, large area samples. In contrast, equilibrium measurements require large separation between the hot and cold ends of the sample to allow ΔT to be maintained.[15–17] In previous work,[3,4] single or small numbers of SiNWs were used, such that the thermal resistance was large and ΔT could be established at equilibrium. As we characterise ~10^7 NWs in parallel, the thermal resistance is reduced, making equilibrium measurements difficult. Figure 2(a) shows our experimental apparatus schematically. The Si sample is sandwiched between a bottom (cold) Cu heat sink (temperature $T1$) and a top Cu "hot" reservoir (temperature $T2$), allowing measurement of the temperature difference $\Delta T = T2 - T1$. Pressure is applied to the top Cu block, and Al foil (thickness 120 μm) is used to improve the Si/Cu thermal contacts. Reduction of the bottom Cu block temperature, and the time lag in the top Cu block reaching this temperature, allows a small transient ΔT to exist across the sample. We then measure simultaneously ΔT and ΔV (open circuit voltage), as a function of time, from the point where $T1$ is constant. Measurements are performed from 300 to 30 K. The temperature sensor at the top Cu block is placed very close (<1 mm) to the sample, allowing measurement of temperature near the sample/Cu interface. In addition, the time constants of the exponential decays for ΔV and ΔT are similar and very long (~10 s or greater). The electron distribution can then adjust as the temperature changes, and quasi-static conditions exist in the sample. This allows the use of equilibrium equations to quantify *S*. We have also performed equilibrium measurements on the NWs at room temperature, which give similar values of *S* to our transient measurements. Finally, we consider the suitability of the top Cu block as a heat reservoir. The heat capacity of Cu ~ 24 J/mol K (Ref. 18) and of Si is ~20 J/mol K (Ref. 19). The mass of the Cu block is 1 g and of the Si sample is 0.1 g. It then follows that the heat stored in the top Cu block is ~9 times greater than in the Si sample.

Figure 2(b) shows measurements for the bulk "parent" Si sample at 160 K. ΔV and ΔT decay exponentially, with similar time constants ~16 s. $S = \Delta V/\Delta T$ is then calculated from the ΔV-ΔT plot slope. Figure 2(b) (inset) shows linear ΔV-ΔT plots for this sample from 280 to 80 K. Figure 2(c) shows similar plots for an 80 μm SiNW sample, from 270 to

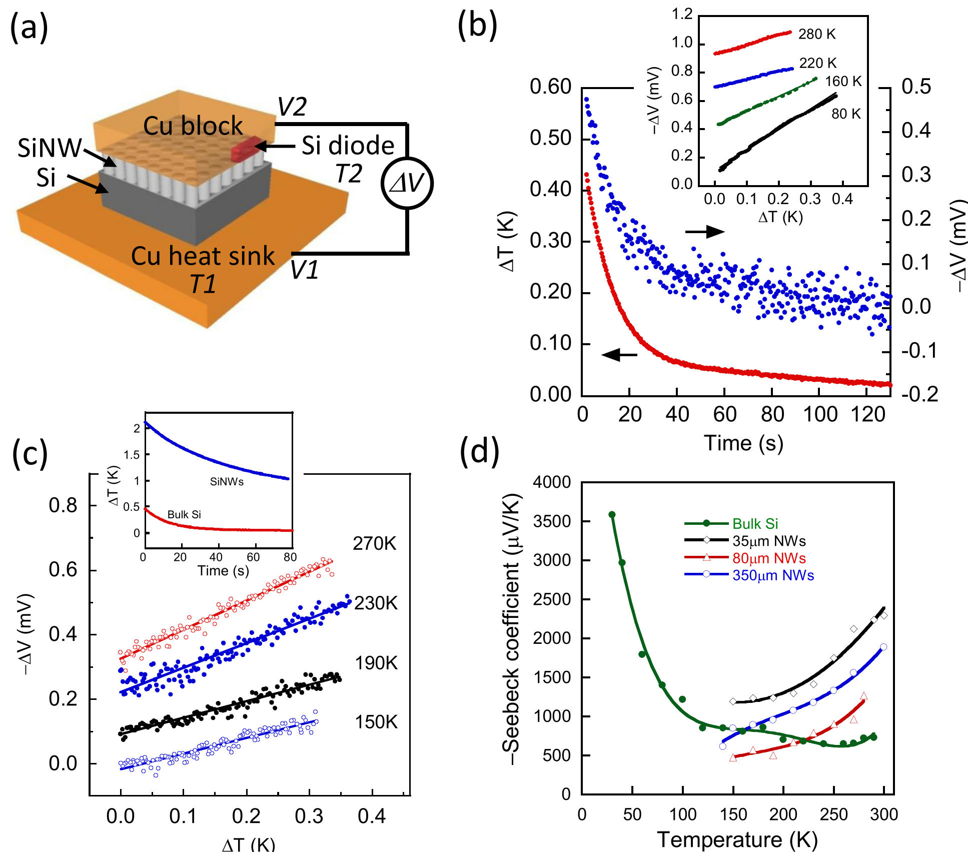

FIG. 2. (a) Schematic diagram of experimental apparatus. The bottom and top Cu block temperatures are $T1$ and $T2$, with temperature difference $\Delta T = T2 - T1$. Voltage difference between the blocks $\Delta V = V2 - V1$. (b) ΔV and ΔT vs. time for bulk Si, at 160 K. Inset shows $\Delta V - \Delta T$, for 280–80 K heat sink temperature. Curves are offset for clarity. (c) $\Delta V - \Delta T$ for 80 μm SiNWs, from 270 to 150 K. Curves are offset for clarity. Inset shows the exponential decay of ΔT as a function of time, for bulk Si and SiNW samples at 160 K. (d) Seebeck coefficient for bulk Si and for SiNW arrays with 35, 80, and 350 μm NW length. The solid lines are a polynomial fits to provide a guide to the eye.

This article is copyrighted as indicated in the abstract. Reuse of AIP content is subject to the terms at: http://scitation.aip.org/termsconditions. Downloaded to IP: 155.198.134.118 On: Tue, 22 Oct 2013 13:01:45

150 K. The inset shows ΔT as a function of time for bulk and SiNW samples at 160 K. Figure 2(d) shows S for bulk Si (S_{bulk}) and for SiNW arrays (S_{NW}) with 35, 80, and 350 μm NW lengths. Measurements were from 290 to 30 K for bulk Si and 300–140 K for SiNWs.

In Figure 2(d), S_{NW} is calculated as follows. We define the equations

$$\frac{\Delta T_{NW}}{\Delta T} = \frac{1}{1 + \Delta T_{bulk}/\Delta T_{NW}}, \tag{1}$$

$$\Delta T_{bulk} \propto \frac{1}{\kappa_B}\frac{L_B}{A_B}; \quad \Delta T_{NW} \propto \frac{1}{\kappa_{NW}}\frac{L_{NW}}{F \times A_B}, \tag{2}$$

$$\frac{\Delta V_{NW}}{\Delta V} = \frac{1}{1 + \Delta V_{bulk}/\Delta V_{NW}} = \frac{1}{1 + S_{bulk}\Delta T_{bulk}/S_{NW}\Delta V_{NW}}, \tag{3}$$

where (ΔV_{NW}, ΔT_{NW}) and (ΔV_{bulk}, ΔT_{bulk}) are the voltage and temperature across the SiNWs and the bulk Si substrate, respectively. Furthermore, ($\kappa_{B,}$ L_B) and ($\kappa_{NW,}$ L_{NW}) are the thermal conductivity and length in the bulk Si and SiNWs, respectively, A_B is the bulk Si surface area, and F is the filling factor of the SiNW array. In our case, $F = 30\%$, while for κ_{NW} and κ_B, we use data from literature.[3,10] Here, κ_{NW} is used only to estimate ΔT across the SiNW and the bulk substrate. In principle, a transient method allows direct measurement of κ_{NW}. However, this would require an estimate of the heat loss from the top Cu block, e.g., through the leads connecting to the block and the temperature sensor. The time constants for bulk (τ_B) and the SiNWs (τ_{SiNW}) are very different, with $\tau_B = 16.8$ and $\tau_{SiNW} = 44.12$ (Fig. 2(c) inset). The ratio of the time constants $\tau_B/\tau_{SiNW} \propto \kappa_{Si}/\kappa_{NW}$ suggests that κ_{NW} is reduced to $\sim 0.38\kappa_{Si}$, a value within the range reported for SiNWs also fabricated by a MACE process.[3] Substituting Eq. (3) into the ratio $S_{NW}/S = (\Delta V_{NW}/\Delta V)/(\Delta T_{NW}/\Delta T)$, where S is the Seebeck coefficient for the entire SiNW/Si bulk sample, and solving for S_{NW}, we have

$$S_{NW} = S\left(1 - \frac{S_{bulk}}{S}\right)\frac{\Delta T}{\Delta T_{NW}} + \frac{S_{bulk}}{S}. \tag{4}$$

Here, $\Delta T/\Delta T_{NW}$ is given by Eqs. (1) and (2), and S_{bulk} and S are given by our measured data. It was not possible to measure the SiNWs below $\sim$140 K, due to increasing sample resistance. At room temperature, $S_{NW} > S_{bulk}$ by up to $\sim$3 times. However, S_{bulk} increases and S_{NW} decreases with decreasing T and at lower T, $S_{NW} < S_{bulk}$ (e.g., at 220 K for the 80 μm sample).

The increase in S_{bulk} is caused by strong enhancement of phonon drag.[10] The decrease in S_{NW} then implies suppression of phonon drag. Typically, $S_{bulk} = S_p + S_d$, where S_p is the phonon drag and S_d is the electron diffusion component. In phonon drag, momentum transfer from phonons to electrons via electron-phonon scattering increases the number of electrons reaching the cold side and therefore S. S_p is large in lightly doped in comparison with heavily doped materials[10] as in the later case, impurity scattering of phonons suppresses S_p.

In lightly doped bulk semiconductors, S_d is given by[20,21]

$$S_d = -\frac{k_B}{e}\left(\frac{E_C - E_F}{k_B T} + \left(r + \frac{5}{2}\right)\right). \tag{5}$$

Here, k_B is the Boltzmann constant, E_F is the Fermi energy, E_C is the conduction band energy, e is the electron charge, and r is a scattering factor, assumed to be -0.5 if phonon scattering of carriers dominates over impurity scattering.[21] E_F can be calculated using[22]

$$n_d\left(1 - \left(\frac{1}{2}\exp\left(\frac{E_D - E_F}{k_B T}\right) + 1\right)^{-1}\right) = n_0 \exp\left(\frac{E_F - E_C}{k_B T}\right). \tag{6}$$

Here n_d is the ionised donor concentration, $E_D = 0.045$ eV is the donor (phosphorous) energy, $n_0 = 2(2\pi m^* k_B T/h^2)^{3/2}$ is the conduction band effective density of states, $m^* = 1.08 \times$ electron rest mass is the electron effective mass, and h is Planck's constant. Finally, S_p is given by[20]

$$S_p = -\frac{\beta v_p l_p}{\mu_e T}. \tag{7}$$

Here, v_p and l_p are the velocity and mean free path of phonons participating in phonon drag, μ_e is the electron mobility, and β characterises electron-phonon interaction. At room temperature and above, phonon-phonon interaction (Umklapp scattering) is predominant and $\beta \approx 0$. This implies that S_p may be neglected at room temperature and $S_{bulk} \approx S_d$. As the temperature is lowered, Umklapp scattering becomes increasingly difficult, leading to $\beta > 0$. At low temperatures,[21] phonon-phonon interaction is almost void and $\beta \approx 1$. Furthermore, as $\mu_e \propto T^{-3/2}$ in lightly doped Si and v_p may be assumed to be constant, we have $S_p T^{-1/2} \propto l_p$, providing a means to obtain the temperature dependence of l_p from S_p.

Figure 3(a) shows S_{bulk} and S_d calculated using Eqs. (1) and (2) for 10^{15}/cm^3 doping concentration, where $S_{bulk} \approx S_d \approx 730$ μV/K at 290 K. S_{bulk} is, however, slightly smaller than S_d from 220 K $< T <$ 300 K, as we may have overestimated S_d if $r < -0.5$ or underestimated S_{bulk} due to unaccounted interface temperature drops. $S_p = S_{bulk} - S_d$ is extracted assuming that S_p is negligible at room temperature. S_p increases below $\sim$250 K and $\sim$80 K, $S_p > S_d$ (e.g., at 30 K, $S_p = 0.7S_{bulk}$). The temperature dependence of l_p is found by plotting $S_p T^{-1/2} \propto l_p$ vs. T on a log-log scale (Fig. 3(a) inset). We find a power-law dependence, with $l_p \propto T^n$ where $n = -2.3$. This is associated with the reduction in Umklapp scattering of phonons with reducing T and is similar to published data,[10] where $n \sim 2.1$. Finally, Fig. 3(b) shows S_{NW}, normalized to room-temperature values, vs. T. All samples show a similar behaviour, demonstrating a "universal" temperature dependence with NW length.

In our lightly doped NWs, impurity scattering of phonons is negligible and cannot suppress phonon drag. This leaves surface scattering due to restricted NW dimensions and surface roughness as the likely suppression mechanism. As $l_p \sim 1$ μm in lightly doped[10] bulk Si at 300 K and increases at lower temperatures (Fig. 3(a) inset), l_p is always greater than NW diameter. Strong surface scattering of phonons in the NWs then limits $l_p \sim$ NW diameter and

This article is copyrighted as indicated in the abstract. Reuse of AIP content is subject to the terms at: http://scitation.aip.org/termsconditions. Downloaded to IP: 155.198.134.118 On: Tue, 22 Oct 2013 13:01:45

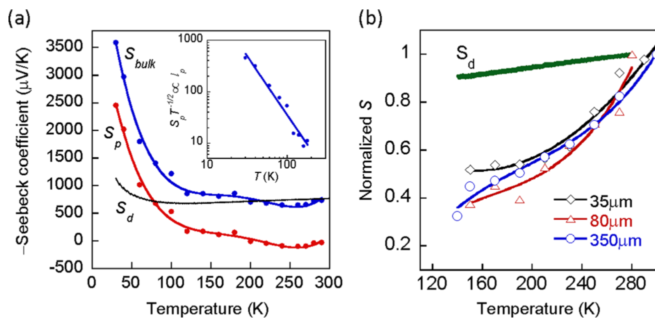

FIG. 3. (a) S_{bulk} (measured), S_d (calculated) and S_p (extracted), vs. T in bulk Si. The inset shows $S_p T^{-1/2} \propto l_p$, the phonon mean free path, vs. T. (b) S_{NW} normalized with the room-temperature values for three samples, vs. T. S_d is shown for comparison.

suppresses S_p. This is the same underlying mechanism for reduced κ in SiNWs,[3,23] implying interdependence between S_{NW} and κ. We also observe maximum $S_{NW} \sim 3S_{bulk}$ at room temperature (Fig. 2(d)). This may be attributed to either a change in r (Eq. (1)) due to the change in scattering mechanism from phonon to surface scattering or an increase in $E_C - E_F$ due to surface effects. Finally, we estimate ZT in the NWs, at 300 K. Using the maximum $S_{NW} = 2300\,\mu$V/K, $\kappa_{NW} = 8$ W/m K (Ref. 3), and assuming σ in the NWs is unchanged from bulk,[24] we find $ZT_{NW} = 0.005 \approx 150 ZT_{bulk}$. This suggests a large improvement in the TE properties of lightly doped SiNWs compared to bulk Si.

The authors would like to acknowledge M. Green, K. Fobelets, C. Li, and V. Stevens for useful discussions and the financial support of the E.ON International Research Initiative.

[1]A. Majumdar, Science **303**, 777–778 (2004).
[2]F. DiSalvo, Science **285**, 703–706 (1999).
[3]A. I. Hochbaum, R. Chen, R. D. Delgado, W. Liang, E. C. Garnett, M. Najarian, A. Majumdar, and P. Yang, Nature **451**, 163–167 (2008).
[4]A. Boukai, Y. Bunimovich, J. Tahir-Kheli, J. K. Yu, W. Goddard, and J. Heath, Nature **451**, 168–171 (2008).
[5]J. R. Drabble and H. J. Goldsmid, *Thermal Conduction in Semiconductors* (Pergamon Press, Oxford, 1961).
[6]G. J. Snyder and E. S. Toberer, Nature Mater. **7**, 105–114 (2008).
[7]M. S. Dresselhaus, G. Chen, M. Y. Tang, R. G. Yang, H. Lee, D. Z. Wang, Z. F. Ren, J.-P. Fleurial, and P. Gogna, Adv. Mater. **19**, 1043–1053 (2007).
[8]M. S. Dresselhaus, G. Dresselhaus, X. Sun, Z. Zhang, S. B. Cronin, and T. Koga, Phys. Solid State **41**, 679–682 (1999).
[9]S. K. Bux, J. P. Fleurial, and R. B. Kaner, Chem. Commun. **46**, 8311–8324 (2010).
[10]L. Weber and E. Gmelin, Appl. Phys. A **53**, 136–140 (1991).
[11]K. Q. Peng, Y. J. Yan, S. P. Gao, and J. Zhu, Adv. Mater. **16**, 1164–1167 (2002).
[12]Z. Huang, N. Geyer, P. Werner, J. de Boor, and U. Gosele, Adv. Mater. **23**, 285–308 (2011).
[13]Y. Qu, L. Liao, Y. Li, H. Zhang, and Y. Huang, Nano Lett. **9**, 4539–4543 (2009).
[14]H. Fang, Y. Wu, J. Zhao, and J. Zhu, Nanotechnology **17**, 3768–3774 (2006).
[15]T. M. Tritt, Mat. Res. Soc. **478**, 25–36 (1997).
[16]T. M. Tritt and V. Browning, Semicond. Semimetals **69**, 25–49 (2001).
[17]*Thermoelectrics Handbook: Macro to Nano*, edited by D. M. Rowe (CRC Press, 2006).
[18]G. K. White and S. J. Collocott, J. Phys. Chem. Ref. Data **13**, 1251–1257 (1984).
[19]C. Kittel, *Introduction to Solid State Physics* (John Wiley & Sons, New York, 1976).
[20]G. S. Nolas, J. Sharp, and J. Goldsmid, *Thermoelectrics Basic Principles and New Materials Developments* (Springer, Berlin, 2001).
[21]H. J. Goldsmid, *Applications of Thermoelectricity* (Methuen & Co., London, 1960).
[22]S. M. Sze, *Physics of Semiconductor Devices* (John Wiley & Sons, New York, 1981).
[23]Z. Wang, Z. Ni, M. Chen, K. Bi, and Y. Chen, Physica B **406**, 2515–2520 (2011).
[24]J. Jie, W. Zhang, K. Peng, G. Yuan, C. S. Lee, and S.-T. Lee, Adv. Funct. Mater. **18**, 3251–3257 (2008).

This article is copyrighted as indicated in the abstract. Reuse of AIP content is subject to the terms at: http://scitation.aip.org/termsconditions. Downloaded to IP: 155.198.134.118 On: Tue, 22 Oct 2013 13:01:45